Supplement

THE DETERMINANTS OF THE ONSET DYNAMICS OF ACTION POTENTIALS IN A COMPUTATIONAL MODEL

Gytis Baranauskas, Albert Mukovskiy, Fred Wolf and Maxim Volgushev

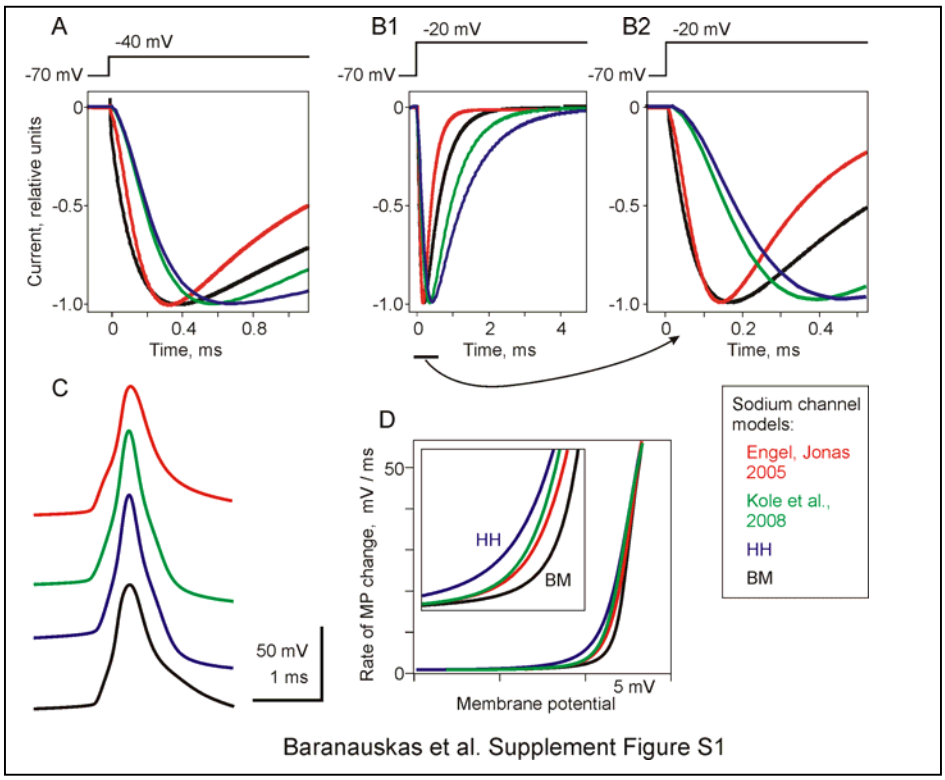

Supplement Figure S1. Sodium currents and action potentials simulated with four models of sodium channels.
A, B: Whole cell currents simulated with 4 different models of sodium channels in response to voltage steps from –70 mV to –40 mV (A) and –20 mV (B). B2 shows a portion from B1 at expanded time scale. The current amplitude is normalized to the peak to facilitate comparison of response dynamics. Note that the BM and Engel and Jonas models generate the fastest current onset for both voltage steps. Note that Engel and Jonas model has fastest inactivation kinetics.
C: Action potentials generated in a multicompartment models with our standard settings (cytoplasmic resistance 150 Ohm*cm; AIS diameter 1.2 µm; density of sodium channels in the soma 100 pS/µm^2), and density of sodium channels in the AIS 50 times higher than in the soma (~5,000 pS/µm^2). All model settings were the same but for the model of sodium channels implemented.
D: Initial portion of the phase plots of 4 APs from C; inset shows part of the same traces at expanded scale. Traces in D are aligned at their beginning and at their end point to facilitage comparison of onset dynamics. Note that AP generated with the BM sodium channel model has the fastest onset, AP generated by the HH model has the slowest onset, and APs generated by Engel, Jonas and by Kole et al., models exhibit intermediate onset dynamics.

In all panels, the following 4 models of sodium channels were used: 1) Engel and Jonas, 2005, this model was developed to fit the presynaptic sodium current kinetics (Engel, Jonas, 2005 red traces); 2) Kole et al, 2008 model that was obtained by fitting sodium currents recorded in layer V cortical pyramidal neurons (Kole et al., 2008, green traces); 3) Mainen and Sejnowski, 1995 model that was obtained by fitting Hodgkin and Huxley sodium channel model to traces of Huguenard et al, 1989 and Stuart and Sakmann, 1994 (HH, blue traces); 4) Baranauskas and Martina, 2006, (BM, black traces).
All simulations were performed for 32°C.

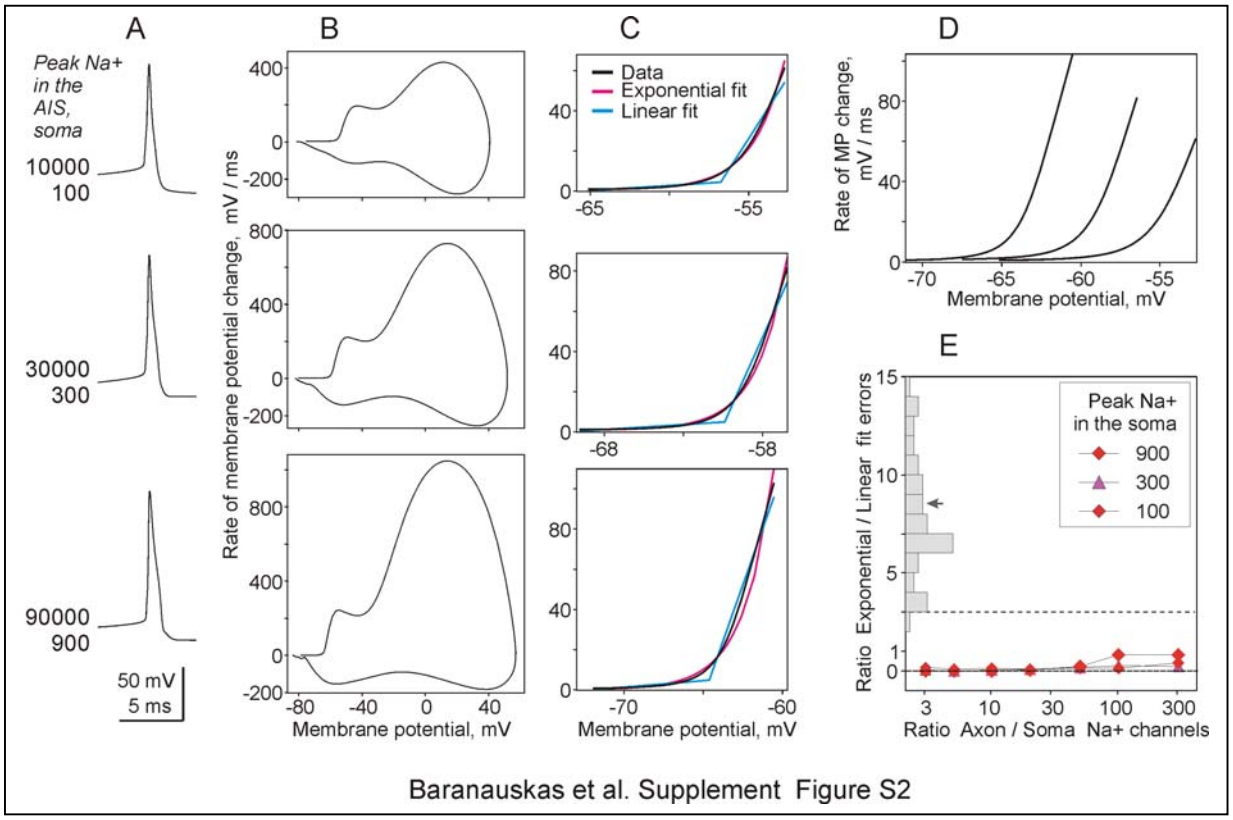

Supplement Figure S2. Onset dynamics of AP in three HH type models with different density of sodium channels in the soma.

A-C: APs generated with the models with the maximal Na+ conductance density in the soma of 100 pS/μm^2, 300 pS/μm^2 and 900 pS/μm^2, as indicated. In all three examples, density of sodium channels in the AIS was 100 times higher than in the soma, and thus gNa in the AIS was 10,000 pS/μm^2, 30,000 pS/μm^2 and 90,000 pS/μm^2. In C, the ratio of errors of exponential to piecewise linear fits were: 0.14, 0.28 and 0.82.

D: Initial portions of AP phase plots of 3 APs from C, superimposed.

E: Dependence of the ratio of fit errors on the ratio of AIS/soma sodium channel density in the three models with low (100 pS/μm^2), medium (300 pS/μm^2) and high (900 pS/μm^2) maximal sodium conductance in the soma.

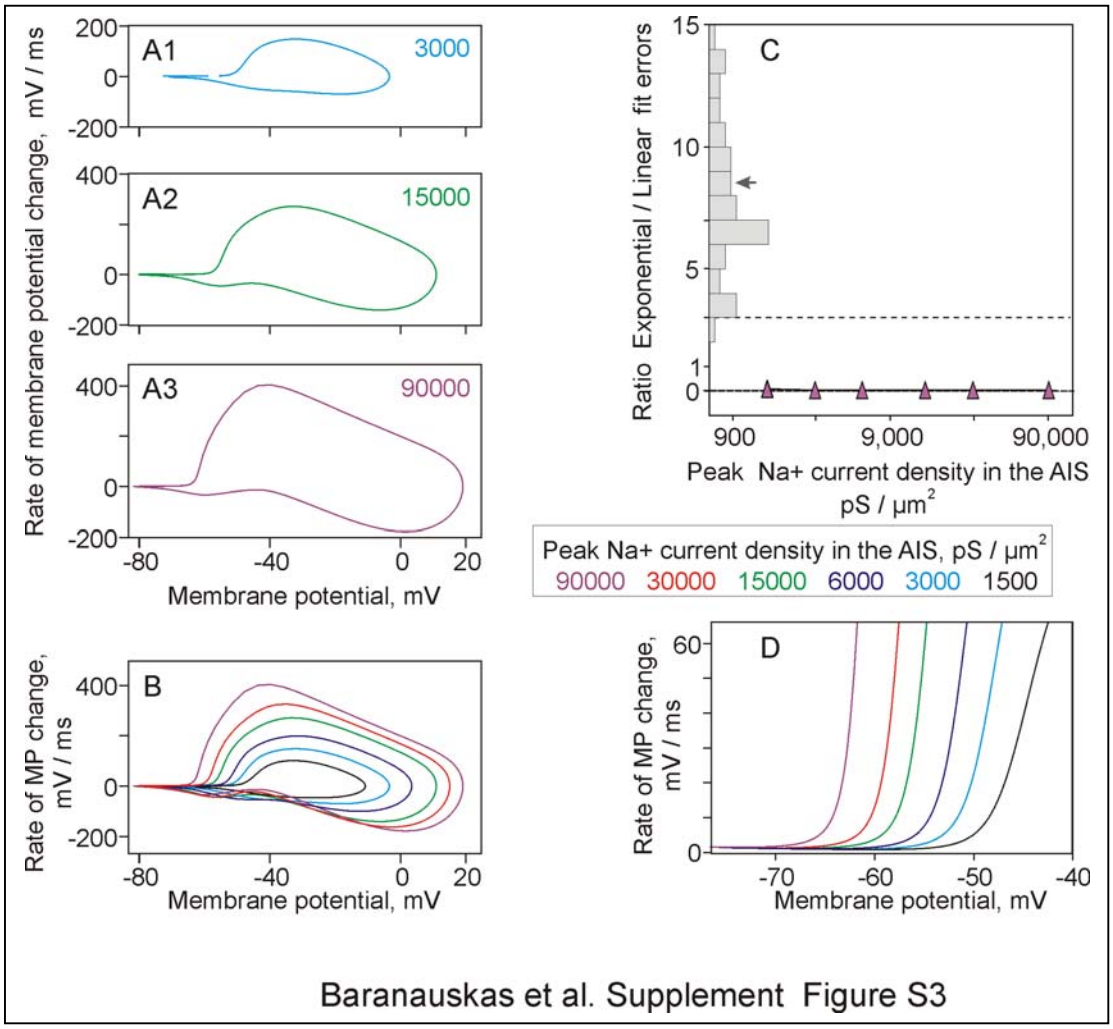

Supplement Figure S3. Onset dynamics of the isolated invasion component in the soma.
To isolate the component of voltage change during the somatic AP that is produced by Iprop, density of sodium channels was set to zero in all compartments but for the AIS (Yu et al. 2008). gNa in the AIS was then systematically varied from 1,500 pS/µm^2 to 90,000 pS/µm^2.
A1-A3: Phase plots of the invasion components in the soma in the models with gNa in the AIS of 3,000 pS/µm^2, 15,000 pS/µm^2 and 90,000 pS/µm^2, as indicated.
B: An overlay of the phase plots of invasion components in models with different peak density of sodium current in the AIS, color coded.
C: Dependence of the ratio of fit errors of the onset dynamics of the isolated invasion component on the peak density of sodium current in the AIS. In all 6 models, the ratio of fit errors was well below 1.
D: Zoom in of the initial portions of the phase plots from B. Color code is the same in B and D.

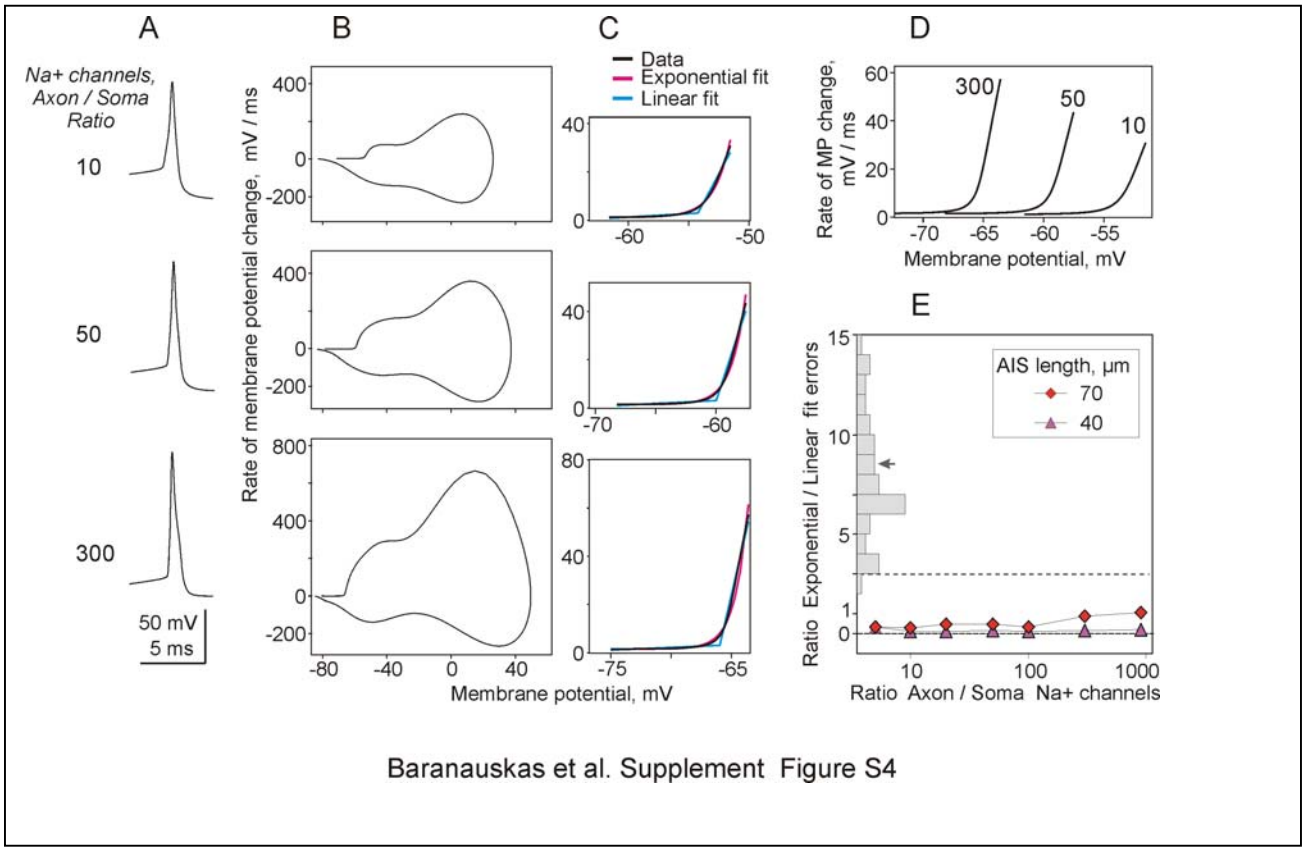

Supplement Figure S4. **AP onset dynamics in a model with a long axon initial segment.**
A-C: AP waveforms, phase plots and zoom in of the initial portion of the phase plots with their exponential and piecewise linear fits in models with HH type sodium channels, having a long (70 µm) axon initial segment. In the examples shown, the density of sodium channels in the AIS was 10, 50 and 300 times higher than in the soma, as indicated on the left. gNa in the soma was 100 pS/µm^2, and thus 1,000 pS/µm^2, 5,000 pS/µm^2 and 30,000 pS/µm^2 in the AIS in the three models. In C, the ratios of fit errors were: 0.22, 0.41 and 0.81.
D: Dependence of the ratio of fit errors on the ratio between AIS/soma sodium channel density for two HH type models, with a long (70 µm) and a regular-length (40 µm) axon initial segment.

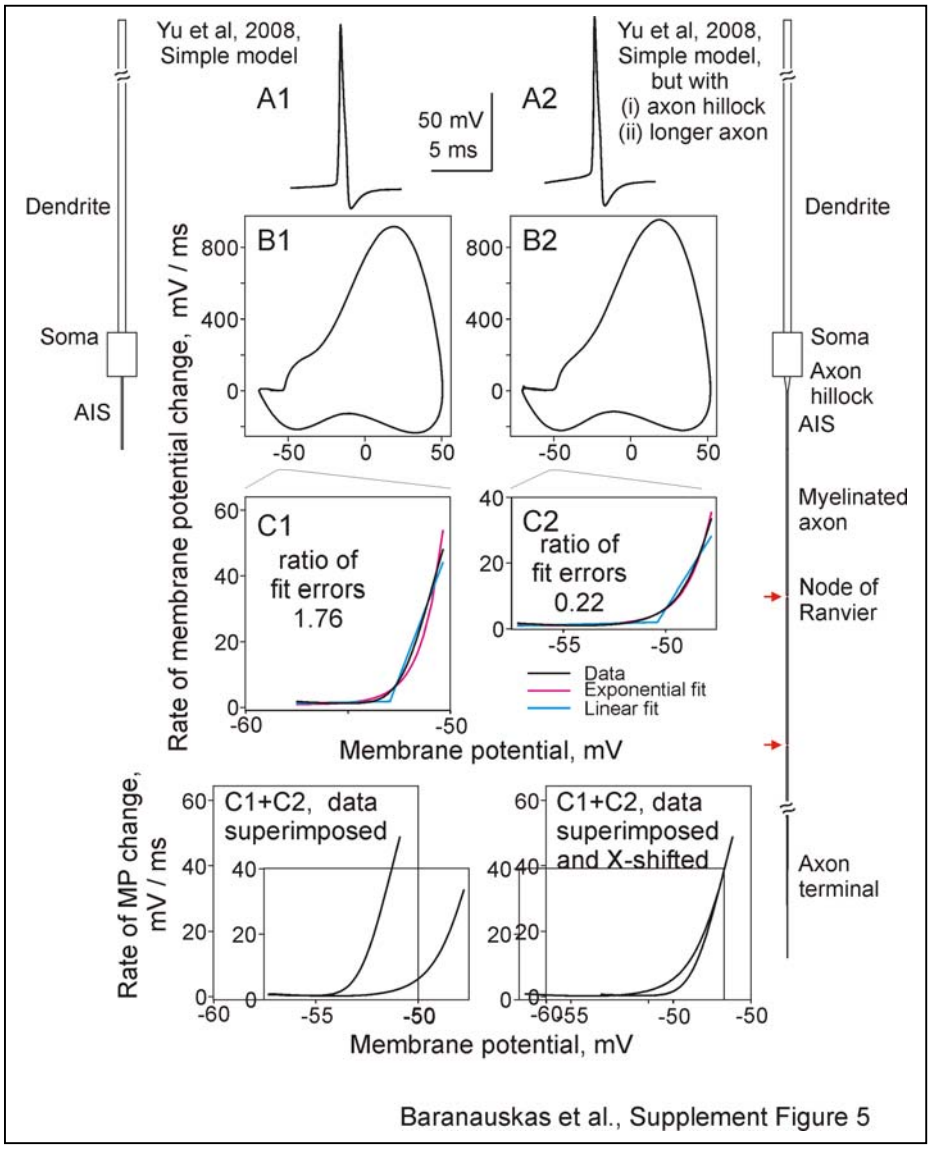

Supplement Figure S5. Fast onset dynamics of somatic action potential in the simple model of spike initiation by Yu, Shu and McCormick (2008) is due to the unusual axon geometry.
A: AP waveforms.
B: Phase plots of APs from A.
C: Initial portion of APs in phase plot at expanded scale, with exponential (magenta) and piecewise linear (cyan) fits.

A1-C1: Somatic AP simulated with the simple model by Yu et al. (2008). Inset on the left shows model geometry. The model, suggested to explain fast onset of somatic APs in large layer 5 pyramidal neurons in the neocortex, consisted of three compartments: a 30x20μm soma, a 1 μm thin 50 μm long axon initial segment attached directly to the soma from one side, and a 5 μm thick 3000 μm long dendrite attached to the soma from the other side. Maximal density of sodium conductance in the soma was 800 pS/μm^2, while in the axon it was 10 times higher, 8,000 pS/μm^2, and in the dendrite 40 times lower, 20 pS/μm^2 (Yu et al. 2008). The AP simulated with this model has fast onset, with the ratio of errors of exponential to piecewise linear fits of 1.76. This value is just approaching the low end of the distribution of fit errors measured for neurons recorded in slices of rat neocortex (Volgushev et al. 2008), see also Fig 9 in the main text.

Since this model ignores morphological features of real axons – the presence of a hillock at the origin of the AIS and extended length of the axon beyond the initial segment, we modified it to a more realistic by (i) extending the axon beyond the initial segment by adding several myelinated segments, nodes of Ranvier and a thin unmyelinated terminal and (ii) reproducing characteristic geometry of the axon hillock by tapering the first 10 μm of the axon from 4 μm to 1

μm (see inset on the right). In accordance with experimental data demonstrating that the density of sodium channels increases towards the distal AIS, but not immediately in the axon hillock (Colbert, Pan 2002; Kole et al. 2008; Lorincz, Nusser 2008), the density of sodium channels in the axon hillock was set intermediate between the soma and the AIS, to 50% of that in the AIS. Thus, in this model the maximal density of sodium conductance in the soma, the hillock and the AIS, was 800 pS/μm^2, 4,000 pS/μm^2 and 8,000 pS/μm^2 . All other settings were the same as in the simple model by Yu et al., 2008.

A2-C2: Somatic AP simulated by the model with the same settings as in (Yu et al., 2008), but with the axon hillock and a long axon (inset on the right). The AP simulated with this model has slow onset, with the ratio of fit errors 0.1. The onsets of APs from C1 and C2 are superimposed in the lowermost panels. Note that the onset is steeper in the model with unusual axon geometry.

Thus, in the simple model by Yu et al, 2008, the AP in the soma exhibits a sharp onset due to the unusual axon geometry. When the axon is extended beyond the initial segment and the axon hillock is added, the onset of AP in the soma of the same model becomes slow.

References

Baranauskas G, Martina M (2006) Sodium currents activate without a Hodgkin-and-Huxley-type delay in central mammalian neurons. *J Neurosci* 26: 671-684.

Colbert CM, Pan E Ion channel properties underlying axonal action potential initiation in pyramidal neurons. *Nat Neurosci* 5: 533-538, 2002.

Engel D, Jonas P (2005) Presynaptic action potential amplification by voltage-gated Na channels in hippocampal mossy fiber boutons. *Neuron* 45, 405-417.

Huguenard JR, Hamill OP, Prince DA (1989) Sodium channels in dendrites of rat cortical pyramidal neurons. *Proc Natl Acad Sci USA* 86:2473-2477

Kole MH, Ilschner SU, Kampa BM, Williams SR, Ruben PC , Stuart GJ Action potential generation requires a high sodium channel density in the axon initial segment. *Nat Neurosc*i 11: 178-86, 2008

Lorincz A, Nusser Z Cell-type-dependent molecular composition of the axon initial segment. *J Neurosci* 28: 14329-14340, 2008

Mainen ZF, Joerges J, Huguenard JR, Sejnowski TJ. (1995) A model of spike initiation in neocortical pyramidal neurons. *Neuron* 15: 1427-1439

Mainen ZF, Sejnowski TJ (1996) Influence of dendritic structure on firing pattern in model neocortical neurons *Nature* 382:363-366.

Stuart G, Sakmann B (1994) Active propagation of somatic action potentials into neocortical pyramidal cell dendrites. *Nature* 367: 69-72

Volgushev M, Malyshev A, Balaban P, Chistiakova M, Volgushev S, Wolf F. Onset dynamics of action potentials in rat neocortical neurons and identified snail neurons: quantification of the difference. *PLoS ONE* 3: e1962, 2008

Yu Y, Shu Y, McCormick DA. Cortical action potential backpropagation explains spike threshold variability and rapid-onset kinetics. *J Neurosci* 28, 7260-7272, 2008